



SG2215 - COMPRESSIBLE FLOW

Experimental laboratory 1: Compressible pipe flow

Author :

Valentin DUVIVIER

vduv@kth.se

Damien LUSSAN

lussan@kth.se

Under the guidance of :

Jens FREDRICH

André WEINGÄRTNER

April 24, 2020

Contents

1	Introduction	2
2	Mass flow rate - Chocked conditions	2
2.1	Mass flow over pressure	2
2.2	Pressure profile	5
3	Pressure drop characteristics	6
3.1	Pressure throughout the pipe	6
3.2	Mach number throughout the pipe	8
3.3	Comparison theory - experiment	10
4	Mach number distribution across the emerging jet at the pipe exit	12
4.1	Using the isentropic ratio	12
4.2	Using the Rayleigh Pitot tube formula	12
4.3	Results	13
5	Uncertainty assessment on the experimental data	14
6	Conclusion	16

1 Introduction

This experiment and the post process coming with it aims in studying the links existing within pressures and Mach numbers in a pipe at choked condition.

The point is to define how these pressures influence each other and moreover how they are being influenced by the case of a choked flow. The same process is being done regarding the Mach number.

The physical experiment consists in a Venturi tube meant to accelerate the flow, followed by a pipe tube, meant to reach the choked condition at the outlet. For this last one, we measure the intern pressure throughout the tube using 8 sensors disposed along it.

During this post-process, first, the mass flow rate of the flow will be determined. With it, iterations may be used in order to consider more accurate values (see dedicated section). Then, we will take a sight to the impact of choked conditions on the pressure drop and, eventually, we will take a final look to the Mach number by looking to its distribution at the pipe exit.

A brief conclusion will be made recalling the results obtained and the context in which we got them, i.e. the source of error and the assumptions considered.

2 Mass flow rate - Choked conditions

This part is made by opening the file called **Exp1**. Furthermore, it is given that the variables here have been measured at $T_0 = 20^\circ C \approx 293K$.

We have 15 iterations in this file (each column corresponding to an iteration), each one representing the data acquired at a different back pressure p_B . We in fact tested a panel of back pressure, until we reached the choked flow conditions.

Finally, the purpose will be to observe and study how the pressure and the Mach number at the Venturi sections are being influenced by this outlet variable.

2.1 Mass flow over pressure

The mass flow rate is the quantity of flow going through a section (here the Venturi sections) in a unit time. Thus, to get a value for it, we look at the incoming and outgoing flow across time.

An other way to get it is considering the continuity equation, that stipulates that the mass flow rate is constant through a friction-less tube. This formula providing an expression for the mass flow rate, and given in the subject, is the following one :

$$\dot{m} = \rho \times u \times A \rightarrow \dot{m} = \rho_2 \times u_2 \times A_2 \quad (1)$$

with \dot{m} the mass flow, ρ_2 this outlet density, u_2 the flow speed at the outlet and A_2 the outlet section.

We then decided to consider the mass flow using the variables at the Venturi tube outlet.

To go deeper on how the mass flow is calculated, we list below the steps of this sub-part :

- We get M_2 from the pressure ratio $\frac{p_{n1}}{p_{n2}}$. We then assume that the inlet pressure at the nozzle (p_{n1}) is equal to the stagnation pressure (p_0). The equation leading to the Mach number, at the outlet of the nozzle, is then this one :

$$\frac{p_0}{p_2} = \left(1 + M_2^2 \times \frac{\gamma - 1}{2}\right)^{\frac{\gamma}{\gamma - 1}} \quad (2)$$

NOTE : as we consider a friction-less flow, this isentropic relation does stand.

- We then obtain the temperature variable T_2 and ρ_2 assuming our gas to be a perfect gas with an adiabatic behavior (implied by the isentropic flow assumption) :

- We get T_2 from the adiabatic relation $TP^{\frac{1-\gamma}{\gamma}}$:

$$\frac{T_0}{T_2} = 1 + M_2^2 \times \frac{\gamma - 1}{2} \quad \rightarrow \quad T_2 = \frac{T_0}{1 + M_2^2 \times \frac{\gamma - 1}{2}}$$

- We get ρ_2 from the perfect gas equation $PV = nRT$ which itself leads to

$$\frac{P_2}{\rho_2} = rT_2 \quad \rightarrow \quad \rho_2 = \frac{P_2}{rT_2}$$

with R the universal perfect gas constant such that $R = 8.314J/(mol.K)$ and $r = \frac{R}{M} = 287J/(kg.K)$ the specific constant of perfect gas.

Finally, we now have enough information to calculate the mass flow rate. Even though, as we used a numerical resolution, we may be tempted to improve our results by iterating. Indeed, by doing so, we would aim into reducing the error due to the approximation of the numerical scheme.

A way of doing it would be derive a new value for M_1 from the mass flow rate and then manage to get a new value for T_1 as well as P_1 . Then, using our isentropic relation, we get the equivalent for the outlet section (i.e. : ρ_2 , P_2 and T_2) and so forth to get a new mass flow rate. This last variable would then converge to a final value supposedly more precise than the first one.

Nevertheless, if we consider initially a good enough numerical scheme (i.e. a relevant initial guess), these iterations are not necessary anymore. We would then easily agree on the fact that the first value of M_1 is relevant enough to consider that the mass flow rate obtained is consistent.

On our part, we considered the case without iteration using then the function *fsolve* and an initial guess of 0.1 for the Mach number M_1 . This method will show itself relevant if we get in the end a physical solution that verifies the overall behavior from theory.

We plotted below the mass flow rate to see how it behaves in function of the back pressure p_B :

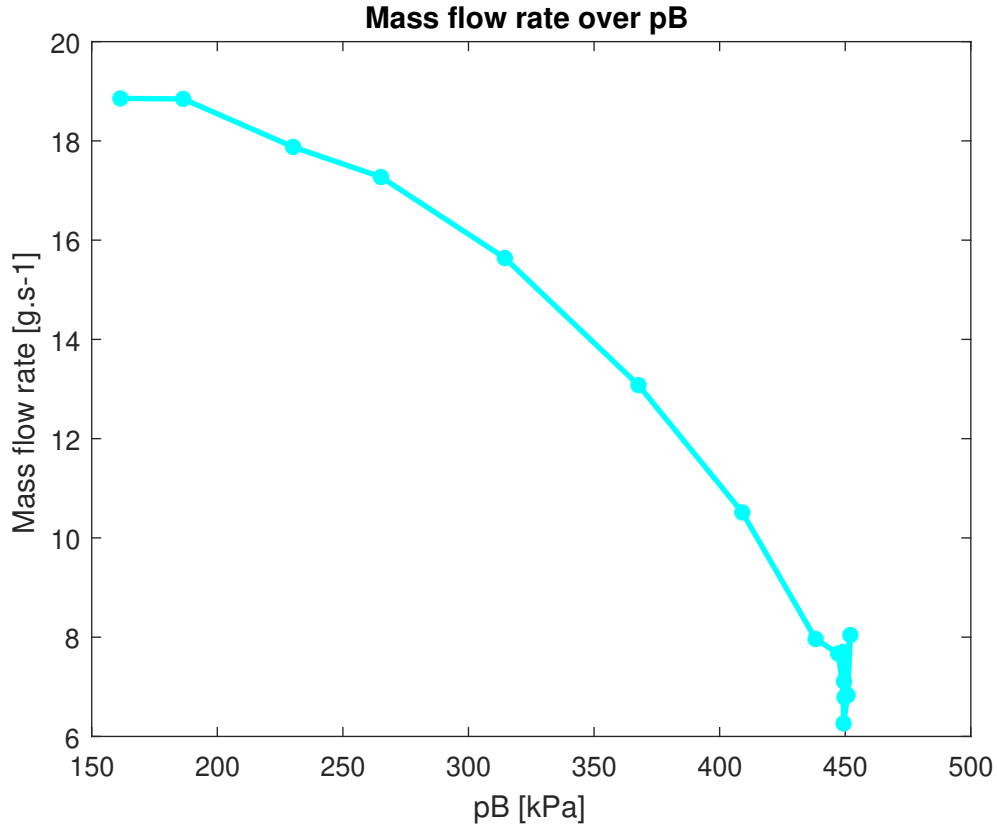


Figure 1: Mass flow rate against the outlet static pressure p_B

In this figure, the key point to consider is that we are diminishing the outlet static pressure and we observe the impact on the mass flow. Thus, we see here that for p_B diminishing, the mass flow is increasing.

In fact, the fluid acts as expected : for a fluid being choked and going toward a lower pressurised environment, we do have its speed that's increasing. Finally, we go from a pressure equal to the inlet pressure $p_0 \approx 450kPa$ and by decreasing p_B we observe an augmentation of the mass flow rate. Even though, this increase tends to get flattened for a low enough p_B . Indeed, we can see that while the mass flow rate continuously increases with the outlet pressure diminishing, there is a point after which it stagnates. This point provides information on the fact that the choked condition might appears close to $150kPa$. We would then get a M equal to 1.

To summarize, we do observe an **acceleration of the flow** when going through the Venturi tube, **and** we have a **constant mass flow** in the end representing a **flow being choked**. By decreasing more the back pressure, this mass flow would stay "frozen" and thus wouldn't evolve anymore.

The back pressure at which we reach the choked condition is close to **150 kPa**.

Now, to finish with this first experiment, we will take a look on how the pressure behaves in the tube.

2.2 Pressure profile

Indeed, we know that it goes from $p_0 \approx 450 \text{ kPa}$ at the inlet to $p_B \approx 100 \text{ kPa}$ at the outlet but we have yet no idea on how the pressure is being modified along the pipe. On the following graph, we plotted the pressures measured throughout the pipe, for the different taps' position.

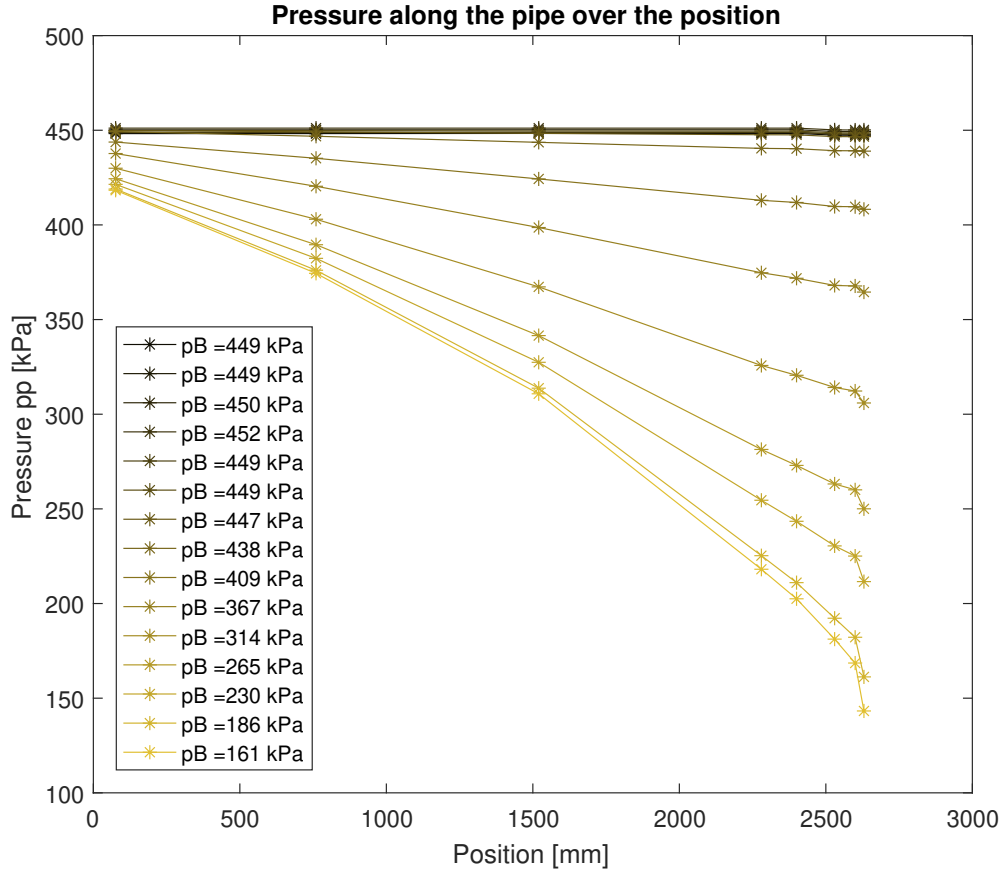


Figure 2: Pressure profile along the pipe for different outlet static pressure

NOTE :

- there is 15 lines, each one representing an iteration ;

- we iterate as we go from $p_0 \approx 450$ kPa to a pressure prone to the apparition of a choked flow. Once again we diminish p_B and observe the repercussion on the flow variables.
- the position is given by the distance between the inlet of the pipe and the position of the tap (bigger the position, closer to the outlet of the pipe and inverse) ;

In a first hand, we clearly observe that the pressure is dropping when getting closer to the pipe outlet. Moreover, this drop is getting bigger as the static outlet pressure diminishes.

Indeed, we recall that we diminish the back pressure to get to the choked conditions and we see what are the repercussions for the pressures in the pipe. We do so 15 times and obtain the above graph.

In fact, it appears on this graph that the pressure on the tube is being influenced by the static pressures at the inlet and the outlet.

When opening the valve, we decrease the pressure p_B , which implies an influence on the tube pressure. Thus, the taps close to the inlet don't suffer a lot the outlet pressure while by going toward the outlet we see that p_B influences more and more the tube's outlet pressures. Besides, the inverse applies : the taps at the inlet are more influenced by the inlet pressure than the outlet pressure.

Eventually, the choked behavior of the flow is matched here and we visually see a drop in the pressure occurring for the taps at the rear of the tube : around 2500 mm while the tube is 2760 mm long.

We thereby have the choked conditions as the outlet as expected. Besides, the associated back pressure to the choked flow is $p_B \approx 150$ kPa.

To summarize, we did **confirm** the previous **observation** made on p_B and we confirm in the same way the fact that the **choked conditions** will appear **at the pipe outlet**.

Now that we have seen the impact of the outlet static pressure on the flow, we will in the next part go deeper in the pressure drop observed above.

3 Pressure drop characteristics

3.1 Pressure throughout the pipe

To study the pressure drop, we use an other file called **Exp2**. In this file, we get the same information than before (p_0 , p_B , p_p , etc) but by considering only the case of choked flow. Thus, we only take a look to a case where the pressure difference between the inlet and the outlet is significant enough to reach $M2 = 1$ at the pipe outlet.

Before displaying the results, we will here expose the equations that led us to the results.

- For the pressure ratio along the pipe, there was no else calculation than the one inherent to the normalized position ;
- For the calculation of the Mach number at each pressure tap, we have been using stagnation state relation for the temperature and a derivative of it for the pressure.

For this last point, the equation used are the following ones :

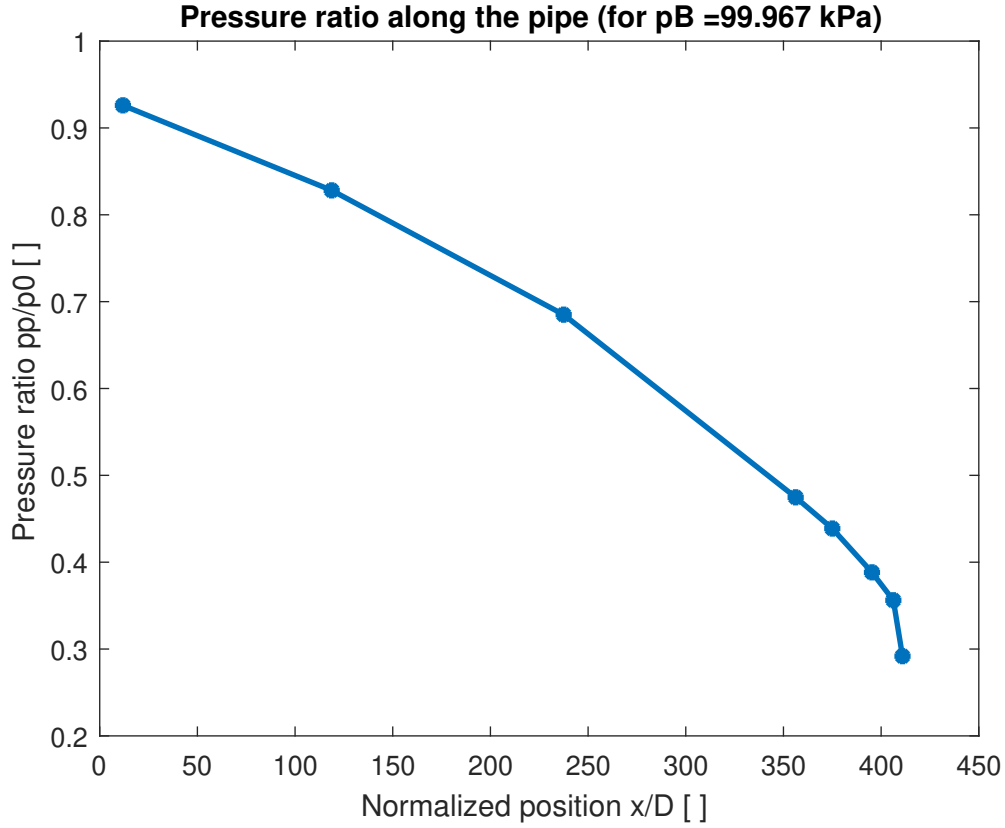
$$\rightarrow \frac{\frac{T_0}{T}}{\frac{T_2}{T_1}} = 1 + \frac{(\gamma - 1)}{2} * M^2 = \frac{2 + (\gamma - 1) * M_1^2}{2 + (\gamma - 1) * M_2^2}$$

By adding the continuity equation to it :

$$\begin{aligned} \rightarrow \frac{P_2}{P_1} &= \frac{M_1}{M_2} \times \sqrt{\frac{T_2}{T_1}} \\ \rightarrow \frac{P_2}{P_i} &= \frac{M_i}{M_2} \times \sqrt{\frac{2 + (\gamma - 1) * M_i^2}{2 + (\gamma - 1) * M_2^2}} \\ \Rightarrow M_i^2(2 + (\gamma - 1) * M_i^2) &= \left(\frac{P_2}{P_i}\right)^2 \times M_2^2(2 + (\gamma - 1) * M_2^2) \end{aligned}$$

As we know every variables except M_i , we have to calculate a determinant that subsequently lead us to a value for the Mach number M_i considering each tap. Note that P_2 stands here for the outlet pressure which is considered as being equal to p_{atm} .

For the graphs, on one hand, the first one shows as discussed the different pressures at each taps :



NOTE : the normalized position provides the distance between the tube's inlet, with respect to the tube's diameter, and each tap's position.

In this graph, we go from an almost unit ratio at the left (inlet of the tube) to a lower one at the outlet. These ratios are made to confirm that the pressure difference considered between the inlet and the outlet during the experiment is big enough to possibly get choked condition. As we see here, we have at the outlet a pressure approximately equal to a third of the one at the inlet.

Moreover, this pressure difference is big enough as we can see a consequent drop around $\frac{x}{D} = 400$. Indeed, while the pressure decreasing is almost linear for the biggest part of the tube, it drops significantly when we approach the end of it.

We thus reach choked condition at the end of the tube for a back pressure close to the atmospheric pressure.

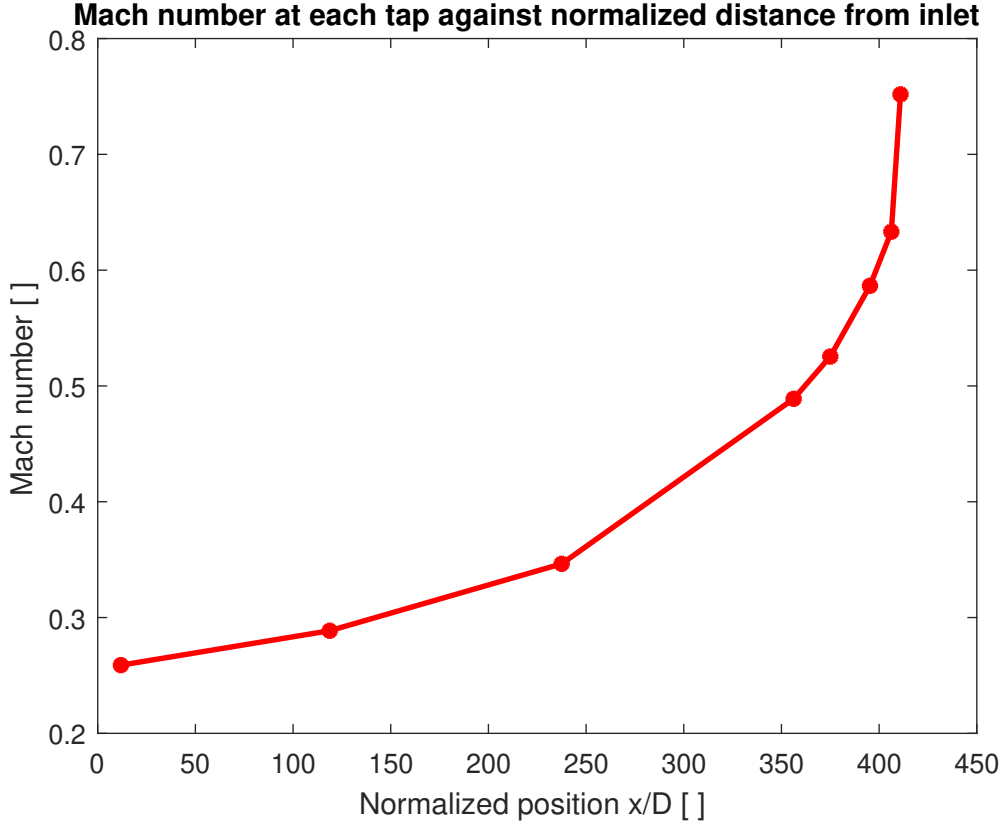
Finally, we see one more time that the pressure at the outlet influences the drop's position.

3.2 Mach number throughout the pipe

Once again we look at the different taps inside the pipe but we now pay attention to the Mach number. More than the value that the Mach number takes, we aim in defining how it behaves by looking to its dependence over the distance from the

inlet of the pipe. We recall that the formula giving the following Mach number is given in the above sub-section.

To have a better idea of what is done here, let's take a look at the following graph :



We first recall that bigger the normalized position is, closer we are from the outlet. Knowing that, we see that the Mach number is increasing with the distance.

First, for what is up to the fact that M is increasing with the normalized distance increasing itself, we see here too that with the pressure decreasing comes an augmentation of the fluid's speed and therefore an augmentation of the Mach number.

For what is up to the values taken by M , it looks like we go toward a choked condition as the Mach number goes from a subsonic behavior toward a supersonic one, but nevertheless, we don't reach $M = 1$. We get close to it though.

Nevertheless, the fact of not reaching the foretold value of 1 isn't a problem. Indeed, the evolution of the Mach number itself is similar to an exponential.

Thus, as we are not at the outlet yet (we are at 2630 mm from the inlet while the outlet is at 2670 mm), we can easily forecast that the Mach number will indeed reach the choked condition within these last few millimeters.

To summarize, the evolution of the Mach number announces that the chocked conditions will be validated at the outlet. The key point here will be to compare this curve with the theoretical one, rather than making sure of reaching chocked condition (as it will be done in section 4).

We will now compare the results obtained here with the one from the home assignment.

3.3 Comparison theory - experiment

The first graph (fig. 3) compares the theoretical and analytical Mach numbers along the pipe.

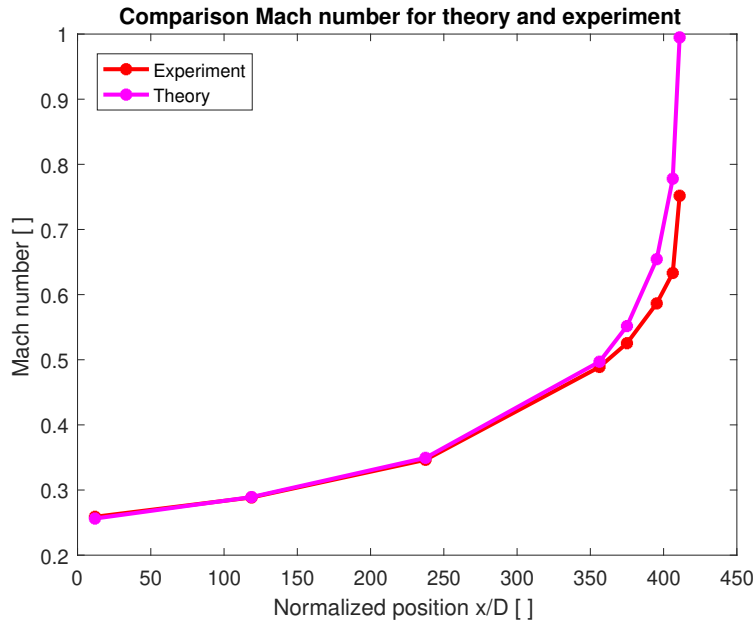


Figure 3: Theoretical and experimental Mach number distribution

In this graph, we see that there is a quasi total superposition between theory and experimentation for more than three fourth of the pipe. Then, a difference appears and we see that while the Mach number is theoretically close to 1 at $x = 2630mm$ (0.9949), it is close to 0.75 for the experimentation.

Thus, a big difference is occurring at the outlet while the error is quiet low for the other considered points.

When we compile our code considering the end of the tube rather than the last tap, we get the following values for the Mach number :

	Theory	Experiment
Mach number	1.00	0.9413

We finally see that the experiment provides values showing a flow really close from chocked condition. Furthermore, the relative error at the outlet is equal to :

$$\frac{\Delta M}{M} = \frac{M_{theory} - M_{exp}}{M_{theory}} \approx 0.06$$

We conclude on the fact that the difference between the experimentation and the theory is still low, even if our results don't show a convergence toward choked condition.

To summarize, as expected and discussed before, the experiment, behaving as an exponential function, will get close to the theoretical value in the end, while it wasn't so sure regarding the above graph.

The discussion of why we don't reach $M = 1$ here as well as a quantification of the error between theory and experimentation is gonna be discussed in the part 4.3.

The second figure (fig. 4) puts in comparison the pressure ratios over the pipe :

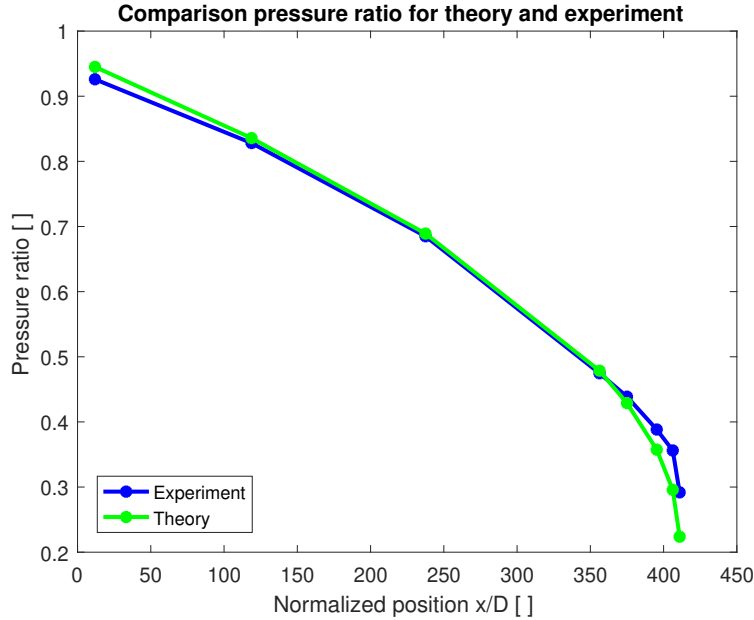


Figure 4: Theoretical and experimental pressure ratio along the pipe

Once again we see that the experiment sticks most of the time with the theory. Where some differences occur is at the top and the rear of the tube, while the curves are quit similar between.

We note that both of them are close to 1 at the beginning, implying that the biggest difference is again appearing at the outlet of the pipe.

Thereby, a scheme that appears into the two above graphs is that, at the extremities, we have a sort of losses that make the actual pressure ratio (respectively the Mach number) lower than the one expected. Therefore, we might be eager to consider the edges of the tube as being prone to a bigger uncertainty.

Here, when we consider the end of the tube rather than the last tap, we have the following results :

	Theory	Experiment
Pressure ratio	0.2225	0.2218

These data lead to the following relative error at the outlet :

$$\frac{\Delta P_{ratio}}{M} = \frac{P_{theory} - P_{exp}}{P_{theory}} \approx 0.03$$

Here too the value of the relative error is close to 0, implying that the experiment will in the end almost reach the theoretical value.

To conclude with this part and these graphs, we see that as seen before the outlet pressure as an impact on the Mach number as well as on the pressure drop. What is to be discussed now is why we have such higher differences at the last tap than at the outlet, by looking to the different considerations being made (see 4.3).

4 Mach number distribution across the emerging jet at the pipe exit

The purpose of the third experiment is to calculate the Mach number distribution in the pipe exit. To do that the outlet valve used in the previous experiments is replaced by a Pitot tube which is not connected to the pipe outlet itself but placed right at the jet exiting from the pipe.

Furthermore the Pitot tube is progressively moved forward into the pipe. The Mach number will be then calculated for each position of the Pitot tube.

4.1 Using the isentropic ratio

One way to compute the radial Mach number distribution is to use the isentropic ratio which is similar to the equation 2:

$$\frac{p_{01}}{p_1} = \left(1 + M_1^2 \cdot \frac{\gamma - 1}{2}\right)^{\frac{\gamma}{\gamma - 1}}$$

with p_{01} corresponding to p_{pitot} in the data and p_1 to all the p_B . From the equation above, the Mach number can be obtained:

$$M_1 = \sqrt{\frac{2}{\gamma - 1} \left(\left(\frac{p_{01}}{p_1} \right)^{\frac{\gamma - 1}{\gamma}} - 1 \right)}$$

4.2 Using the Rayleigh Pitot tube formula

The other way to compute the radial Mach distribution along the emerging jet is to use the Rayleigh Pitot tube formula which is the following:

$$\frac{p_{02}}{p_1} = \left(\frac{(\gamma + 1)^2 M_1^2}{4\gamma M_1^2 - 2(\gamma - 1)} \right)^{\frac{\gamma}{\gamma - 1}} \frac{1 - \gamma + 2\gamma M_1^2}{\gamma + 1} \quad (3)$$

where p_{02} corresponds to p_{pitot} as well. From the previous equation, M_1 should be plotted, but it cannot be easily isolated in the equation. One way to proceed is to use a MATLAB function such as `fsolve` or `vpasolve`.

4.3 Results

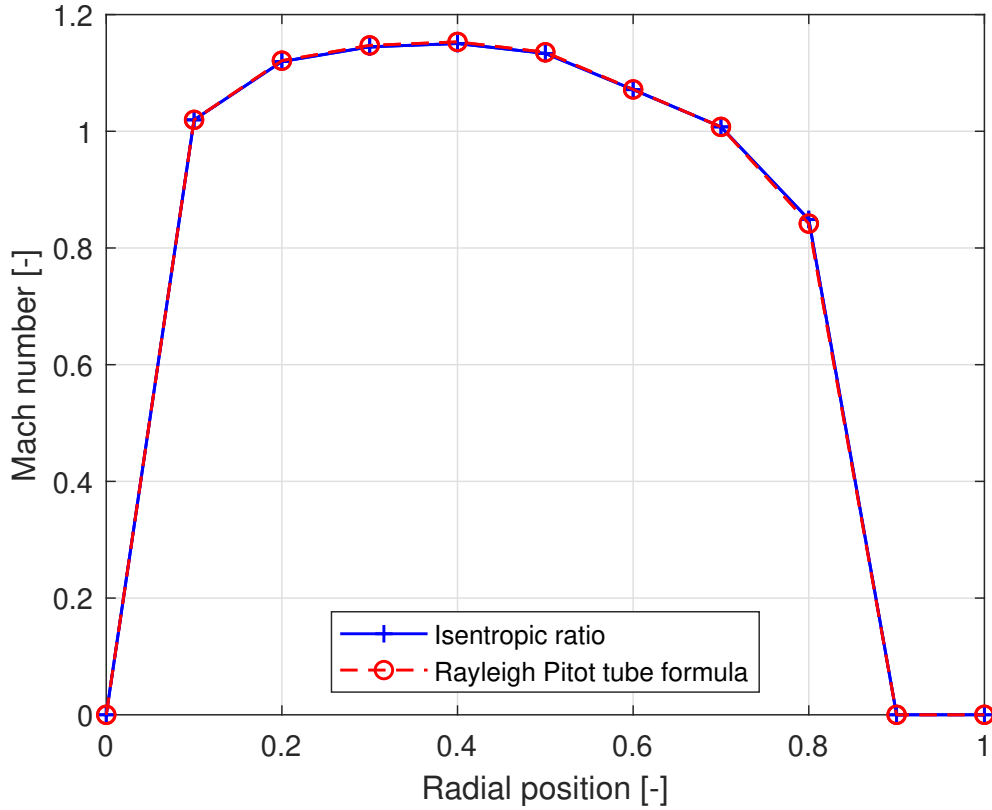


Figure 5: Radial Mach number distribution using both formulas

From figure 5, the Mach number is greater than 1 for most part of the area studied. When it is zero, it's because the Pitot tube is not placed into the pipe yet. The peak is reached around a radial position of 0.4, so it seems that this position is the most consistent one with respect to the pipe outlet.

It can be seen that the results are very close between the isentropic ratio and the Rayleigh Pitot tube formula. The only difference that can be seen on the graph is at the radial position of 0.8 where there is a slight difference. It probably comes from the fact that the Rayleigh Pitot tube formula seems to not be defined for a Mach number below 1 according to the figure 2 in the Lab PM.

The result are in agreement with the figure just referenced, by using both equations the results are supposed to be close for a Mach number range from 1 to 1.25. A significant difference would appear for values beyond. For more specification on the error between the two method is gonna be discussed.

5 Uncertainty assessment on the experimental data

Some of the resolutions has not been made analytically but numerically in particular for the Mach number in the section 3, which will obviously generate some uncertainties in the result.

This fact is considered as being the biggest part for the uncertainties. Indeed, even a part of the error can be due to the material, for what is up to the post-process, it is evident that the type of resolution used will present the biggest influence in term of precision.

To compare the experimental data and the theoretical values of figure 3, the relative error of the Mach number $\frac{\Delta M}{M}$ and the pressure ratio $\frac{\Delta p_{ratio}}{p_{ratio}}$ should be calculated and plotted.

First, we have here the formula used to determine the errors :

$$\frac{\Delta M}{M} = \frac{|M_{\text{measured}} - M_{\text{theoretical}}|}{M_{\text{theoretical}}} \quad (4)$$

$$\frac{\Delta p_{ratio}}{p_{ratio}} = \frac{|p_{ratio, \text{measured}} - p_{ratio, \text{theoretical}}|}{p_{ratio, \text{theoretical}}} \quad (5)$$

The associated curves that we look at are respectively (i.e. same order of appearance) as follows :

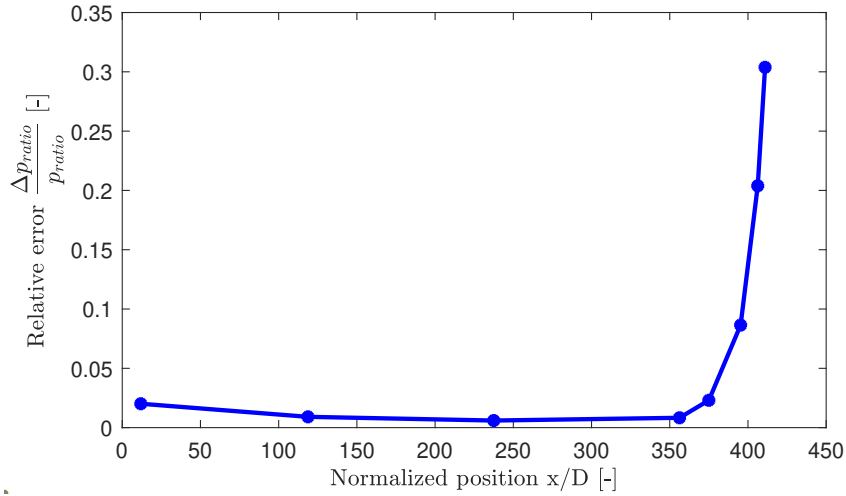


Figure 6: Relative error of the pressure ratio distribution along the pipe

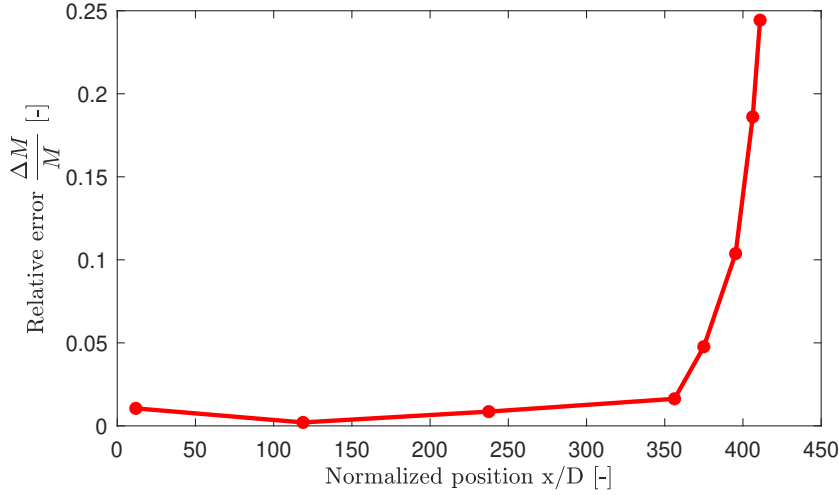


Figure 7: Relative error of the Mach number distribution along the pipe

For both figures 7 and 6, the result of the experiment seems quite close to the theoretical one at least at the beginning of the pipe so at this point it matches quite well. However, it begins to differ quite significantly close to the end of the pipe. The experimental values are then lower.

We here show more significantly the fact that the biggest error occurs at the last tap.

Some factors that can explain these differences can be the sensors that are not precise enough or even the fact that the numerical values are not consistent enough in the sense that the initial guess x_0 wasn't the best one to consider.

On the last experiment (section 4), the difference between both formulas used can be seen by first computing ΔM_1 by using a similar equation to the absolute error and then plotting it.

$$\Delta M_1 = |M_{1,\text{isentropic ratio}} - M_{1,\text{Rayleigh Pitot}}|$$

We then get :

By looking at figure 8, the same conclusion as in the section 4.3 can be made, the difference is almost unnoticeable except for the radial position 0.8.

To summarize, we thereby have here two method that are providing comparable result in this study. Besides, we see that the results differ with the one provided by the part 2. Indeed, it is here clear that the choked condition is reached as we have $M \geq 1$ ($M = 1$ is sufficient though).

We can then conclude on the fact that it is necessary when looking at the end of the tube to make an other approach and doing so to take a better look to a defined position.

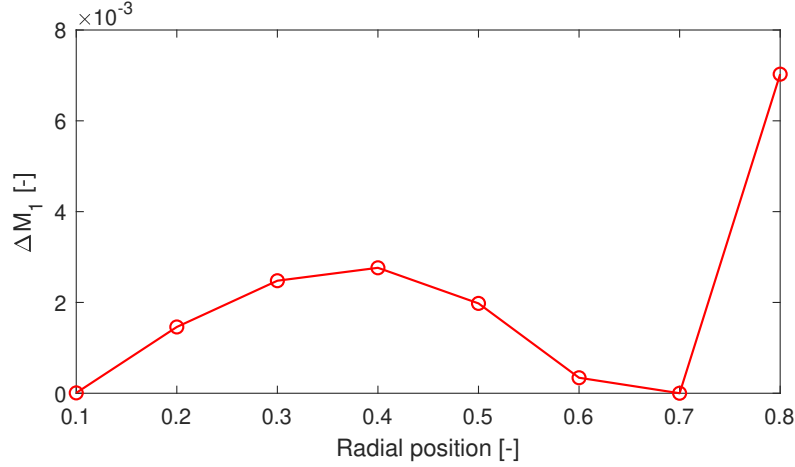


Figure 8: Difference between the Mach number using the isentropic ratio and the Rayleigh Pitot tube formula along the pipe outlet

6 Conclusion

This brief conclusion is made to recall the results seen in this report and to put then one last time in link with their context.

In a first part, we have been using a numerical approach in the home assignment and the part 2. These part being put in comparison, the error due to the numerical approach might cancel each other or at least to reduce each other influence. Thereby, the results gathered in the comparison plots from part 2 present mainly the fact that some losses are observed at the outlet. We recall that the difference between theory and experimentation is almost reduced to a peak in the error at the last tap as the values before and after present a high rate of similitude.

In a second part, we have been seeing an other way to take a look to the chock at the outlet. We used two different formulas and derived associated plots. Once those curves were superposed and that the error graph had been made, it was clear that the two method present a high degree of resemblance. Moreover, this last part permitted us to see that we did reach a sonic flow at the outlet as the theory told us.